

# Realizing and disseminating the SI micronewton with the next generation NIST electrostatic force balance

Jon R. Pratt, David B. Newell, John A. Kramar, and Richard M. Seugling  
National Institute of Standards and Technology, Gaithersburg, MD 20899

## Introduction

The NIST Electrostatic Force Balance (EFB) compares deadweight and mechanical probe forces to an SI realization of force derived from measurements of the capacitance gradient and voltage in an electronic null balance. In the following abstract, we briefly review recent upgrades to this device and present initial results of inter-comparisons between deadweight and electrical forces at levels of 20  $\mu\text{N}$  and 200  $\mu\text{N}$  in a  $10^{-4}$  Pa vacuum environment. The SI calibration of a secondary microforce standard at NIST is revisited; a topic that was described for the first time in the proceedings of the ASPE Winter Topical meeting of January of 2003[1]. Here, we update the status of that work, focusing on the use of this standard in a calibration experiment recently completed in the Physics Department at Worcester Polytechnic Institute (WPI) [2]. This represents our first experience with disseminating SI force at the micronewton level to a user outside of NIST. Certain commercial equipment, instruments, or materials are identified in this article in order to specify the experimental procedure adequately. Such identification is not intended to imply recommendation or endorsement by the National Institute of Standards and Technology, nor is it intended to imply that the materials or equipment identified are necessarily the best available for the purpose.

## Updates to the EFB

The EFB has four major components that have been updated from the original system [e.g., 3-5]. Briefly, these major components are the suspension, the electrostatic force generator, the displacement measuring interferometer, and the vacuum enclosure, as shown schematically in Figure 1.

The rectilinear spring of the original balance suspension has been replaced by a counterbalanced parallelogram linkage that employs a series of cross-flexure pivots as described in [6]. This new mechanism addresses two perceived shortcomings of the original balance. First, it produces a well-constrained motion axis, easily aligned to gravity that is far less susceptible to off-axis forces. Second, it achieves an on-axis stiffness that can be varied to as small as 0.01 N/m through the use of a novel tensioning spring. With on-axis stiffness less than 1 N/m, sub-nanonewton force resolution is possible given realistic null position resolution on the order of nanometers.

A new interferometer [7] replaces the original column-referenced arrangement, removing a potential source of Abbe' measurement error in the determination of the capacitance gradient. This displacement metrology helps ensure determination of the gradient at a relative uncertainty below parts in  $10^5$ . In order to accommodate the beam pattern of this new interferometer, however, the electrodes that comprise the electrostatic force generator required modification. The nominal diameter of the cylindrical capacitor has been increased from approximately 15 mm to 20 mm, with the overall geometry redesigned to preserve

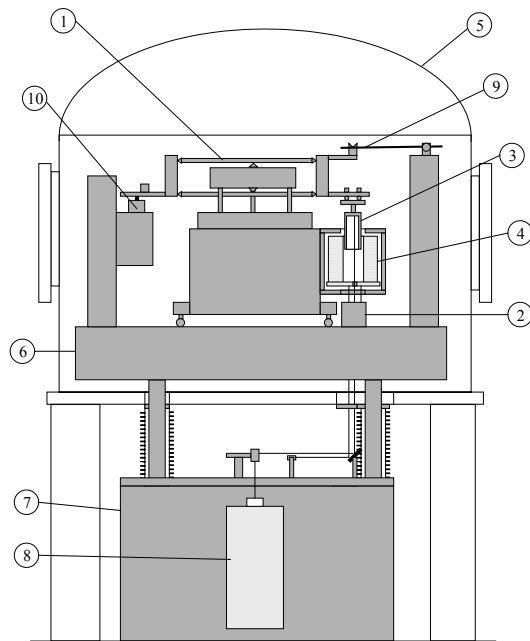


**Figure 1.** Schematic of balance components:  
1) Parallelogram balance 2) Differential plane mirror interferometer 3) Main inner electrode (cross-section) 4) Main outer electrode (cross-section) 5) Vacuum chamber 6) Optical table 7) Granite foundation block 8) Heterodyne laser light source 9) Mass lift 10) Counterweight electrodes

the nominal 1 pF/mm vertical gradient. The inner electrode now also includes a tip/tilt mount between it and the suspension. Previously, a correction was required to account for a cosine error between the interferometer axis and gravity. Now, the interferometer, suspension, force generator, and gravitational axes can all be adjusted into precise alignment with no need for correction.

Finally, the entire experiment has been reassembled on a custom optical table in a specially designed free standing vacuum chamber. The chamber consists of a collar approximately 1 m in diameter and 0.5 m in depth with

a bell jar approximately 0.5 m in height. The optical table on which the EFB is mounted sits on three legs that protrude from the chamber floor through flexible bellows that terminate in blank flanges. These table legs are supported from below the chamber by a large granite block that forms a raised foundation in the space between the chamber legs, as indicated schematically in Figure 1. Thus, the only contact between the vacuum chamber and the experiment is through the relatively compliant bellows. The move to vacuum removes convective air currents that tend to perturb the now large and compliant balance suspension. Also, operation in vacuum eliminates the need to correct for variations in the index of refraction and the permittivity of free space, both of which are a function of the ambient pressure, temperature, and humidity when making measurements in air.

### Operating principles

The EFB generates electrical forces in response to loads along the balance axis that may be calculated from

$$F = \frac{1}{2} \frac{dC}{dz} (U_1^2 - U_2^2) \quad (1)$$

where,  $F$  is the force in nN,  $dC/dz$  is the capacitance gradient in pF/mm, and  $U_1$  is the voltage applied to the outer electrode in V before loading and  $U_2$  is the voltage applied to the outer electrode in V after loading. The balance has two modes of operation, namely a gradient calibration mode and a weighing or force comparison mode.

Gradient calibration is accomplished by moving the balance suspension through a small range of motion (typically  $< \pm 0.2$  mm) about the null position. A second electrode pair on the counterweight side of the balance is used to drive the balance arm, moving the main inner electrode with respect to the fixed main outer electrode. The capacitance and displacement between the fixed and moving electrodes are recorded, so that the general function  $C(z)$  is mapped at discrete locations along the balance motion axis. The function  $C(z)$  is plotted, and then fit with a straight line from which the gradient, or local slope is determined.

Weighings and force comparisons are accomplished by controlling the voltage on the main electrodes to maintain the null position of the balance. A mechanical imbalance is first introduced on the counterweight side, tipping the balance from its rest position and causing the balance feedback control to apply a bias voltage to restore null. Loads can then be measured on the weighing side of the balance, provided they do not exceed the initial bias. Typically, loads are applied and removed and a force calculated from the change in controlled voltage necessary to maintain null.

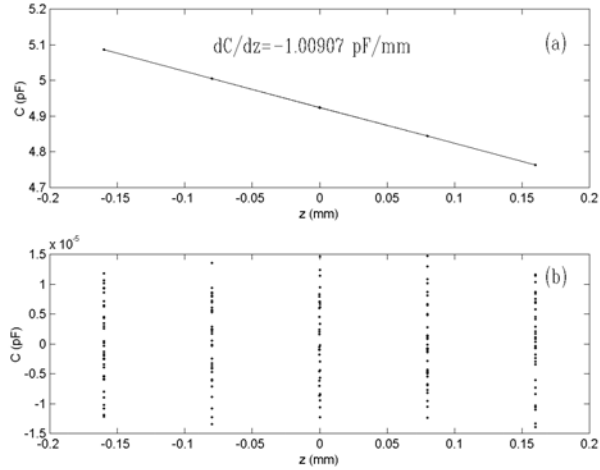


**Figure 2.** Capacitance gradient data: (a)  $C(z)$  and (b) residuals after removal of linear curve fit

**Table 1.** Gradient and weighing results (one standard deviation uncertainties in parantheses)

Date	T(°C)	$dC/dz$ (pF/mm)	# in set	$F_{ef}$ (μN)*	# in set	$F_{mf}$ (μN)	$\left(\frac{F_{ef}}{F_{mf}} - 1\right) \times 10^{-4}$
6/25/04		1.009089(13)	5				
6/25/04				20.0088(8) <sup>+</sup>	300	20.0222(15)	-6.7
6/27/04	22.84(3)	1.009084(15)	180				
6/27/04	22.80(4)			20.0205(7) <sup>ac</sup>	380	-	-0.85
6/28/04	22.74(2)			20.0096(7) <sup>+</sup>	100	-	-6.2
6/28/04	22.73(2)	1.009069(14)	18				
6/28/04	22.3(1)			20.0205(7) <sup>ac</sup>	290	-	-0.83
6/29/04	22.18(4)	1.009072(19)	130				
7/2/04	21.68(2)			196.063(3) <sup>-</sup>	12	196.0125(8)	2.6
7/2/04	21.70(2)			195.947(4) <sup>+</sup>	12	-	-3.3

\*Superscripts indicate dc voltage polarity or that amplitude modulated ac voltage was used

### Gradient data and force comparison experiments

A typical measurement of the capacitance in vacuum as a function of displacement from null is shown in Figure 2, along with a plot of the residuals as a function of displacement after removal of a straight-line fit to the data. The data consist of eighteen complete scans of the inner electrode from  $z = 0.16$  mm to  $z = +0.16$  mm and back again using four equal increments of displacement. The counterweight electrodes drive the balance arm, using the interferometer for position feedback control, performing a move and hold that fixes the relative displacement at each point to within a few nanometers. A precision capacitance bridge then measures the capacitance between the main inner and outer electrode (on the weighing side) while the counterweight electrodes hold the balance still. The averaging time required by the capacitance bridge in order to achieve six significant figures is approximately 40 seconds and sets the speed at which data is collected. Typically, a single scan was completed within 8 minutes. Each of the eighteen scans was fit with a straight line in a least squares fashion from which a slope was determined. The average value of the slopes was 1.009069 pF/mm, with a standard deviation of  $1.4 \times 10^{-5}$  pF/mm. The temperature throughout this experiment was 22.73 °C and deviated by less than 0.02 °C over the entire run.

Deadweight artifacts of nominally 20  $\mu$ N and 200  $\mu$ N were fashioned from stainless steel wire for the weighings. Values for the deadweight masses were determined using the average of ten mass readings taken by placing the deadweight on and off a precision mass microbalance ten times. The deadweight load was computed from the product of this mass and a value for gravity of 9.80103 m/s<sup>2</sup> that was derived from knowledge of the laboratory elevation with respect to a local gravity reference point elsewhere on campus. Load values were 20.0222  $\mu$ N  $\pm$  0.0015  $\mu$ N and 196.0125  $\mu$ N  $\pm$  0.0008  $\mu$ N respectively, where the stated uncertainty is merely one standard deviation of the ten determinations. These measurements remain to be confirmed by the NIST mass group, though the absolute accuracy is expected to be within 5 parts in 10<sup>4</sup> for the small mass and 5 parts in 10<sup>5</sup> for the larger, based on the microbalance specifications. Separate weighing series for each artifact were performed at vacuum using the EFB. Each artifact was lifted on and off the EFB using an automated lift. The force required to maintain the null position of the balance was computed based on equation one. Results from a variety of weighing series are listed in Table 1. Voltage polarity was swapped in some experiments, and an amplitude-modulated, 1 kHz control voltage was used in others, as identified by the superscripts on the electrical force values reported in Table 1.

### Discussion of weighing discrepancies

Electrical forces resulting from the application of positive polarity dc control voltages were consistently less than mechanically determined values; whereas negative polarity voltage resulted in an electrical force value that was greater than expected. Interestingly, the amplitude modulated ac data obtained during 20  $\mu$ N weighings produced agreement within experimental uncertainty. An explanation of these observations is that the inner and outer electrodes themselves generate a potential due to variations in the work functions at the respective electrode surfaces, for instance due to differences in the polycrystalline structure of the two conductors, or differences in the adsorbed elements and compounds on the two surfaces [8]. In this case, the electrostatic force between the electrodes must be characterized as

$$F = \frac{1}{2} \frac{dC}{dz} (U_1^2 - U_2^2 + 2V_s(U_1 - U_2)) \quad (2)$$

where  $V_s$  is the potential difference between the electrodes resulting from the hypothesized surface field effects.

The influence of such a potential can be easily detected by reversing the polarity of the applied voltage, as evidenced by the 200  $\mu$ N data of Table 1: where for a positive polarity, the electrostatic force was 195.947  $\mu$ N while for a negative polarity it was 196.063  $\mu$ N. Clearly, taking  $U_1 \approx 800$  V and  $U_2 \approx 500$  V in equation (2), a bias voltage on the order of 0.19 V is present, though its origin cannot conclusively be linked to the hypothesized surface potential effects. Adopting a technique traditionally used to identify surface potentials and patch fields [8], we have oscillated the main inner electrode as if it were a Kelvin probe. We observed a very small current  $i = V_s dC/dt = V_s dC/dz dz/dt \approx 0.2$  pA as the counterweight electrodes were used to drive the balance through a 0.7 mm p-p sinusoidal oscillation of frequency  $\nu = 0.4$  Hz. Knowing  $dC/dz$ , and approximating  $dz/dt$  by  $2\pi\nu(0.7) \sin 2\pi\nu t$  mm/s, this far coarser measurement yielded  $V_s \approx 0.12$  V—confirming the presence of a surface potential.

### Secondary artifact calibration and dissemination

Two piezoresistive cantilever force sensors were calibrated using the new EFB with the vacuum chamber sealed, but not evacuated. The procedure was similar to that described in [9]; here, a vertical scan stage replaced the lifting fork of Figure 1 and was employed to press the cantilevers against a 1 mm diameter polished ruby sphere that was affixed to the EFB weighing pan. The cantilever force sensitivities were computed using slopes taken from straight-line, least squares approximations to a set of force versus resistance response curves (e.g., as in [1] and [9]). The

sensitivities were  $197.7 \text{ nN}/\Omega \pm 1 \text{ nN}/\Omega$  and  $260.7 \text{ nN}/\Omega \pm 2 \text{ nN}/\Omega$ , where the uncertainties are simply one standard deviation of the respective calibration sets.

These transfer standards were packaged and transported to WPI, where they were employed as reference artifacts in a series of experiments described in detail in [2]. Briefly, the work described in [2] compares three methods that are available for determining AFM cantilever stiffness: namely thermal, geometric, and loading. Of concern here was the loading method, where a transfer standard was placed on the sample stage of an AFM at WPI, and an uncalibrated cantilever was brought into contact with it. The resistance change of the force transfer standard was measured while the AFM scanner was being ramped with the photodiode voltage change being monitored. The WPI researchers were interested in calibrating the unknown cantilever stiffness, rather than its force sensitivity, as suggested in [9], so the photodiode voltage was converted into a deflection rather than directly into force, by probing the unknown against a stiff sample, immediately before or after contact with the transfer standard. The calibrated displacement of the scanner provided the transfer mechanism to convert the photodiode voltage signal into appropriate units of length. Having characterized both displacement and contact force, the unknown stiffness was computed. Agreement among the different stiffness calibration methods was impressive, with all techniques yielding values for the unknown cantilever stiffness well within 10% of each other [2].

### Conclusions

The NIST EFB has been successfully updated and operated in vacuum. Previously unexplained discrepancies between gravitational force and electrostatic force, observed using an earlier version of the balance [3-5], persist with the new balance, but this time a source of the error has been identified along with a corrective experimental procedure. These breakthroughs were possible because of the enhanced stability and precision of the new balance. Convincing evidence that a bias potential exists between the EFB electrodes was drawn from two weighings differing only in voltage polarity, but producing a swing in force of 90 nN. Further investigation is required, but the hypothesized surface field effects seem a very likely source of this discrepancy. The mean value of the two electrical forces agrees well with the redundant cross check provided by the mechanical load, and it suggests that accurate electrical forces can be measured by simply employing a reversal technique to remove the bias.

### Acknowledgements

We thank Dr. Nancy Burnham and her student Eric Thorsen for their participation in this work. Thanks also to various reviewers, colleagues, and visitors for suggesting the amplitude modulated, ac control voltage.

### References

1. Jon R. Pratt, David Newell, John Kramar, Jonathan Mulholland, and Eric Whinton, 2003, "Probe-force calibration experiments using the NIST electrostatic force balance," *Proceedings of the American Society for Precision Engineering 2003 Winter Topical Meeting*, University of Florida, pp. 64-69.
2. G.A. Matei, E.J. Thorsen, J.R. Pratt, D.B. Newell, and N.A. Burnham, "Thermal Method of Cantilever Calibration over a 200 kHz Bandwidth", submitted to *Nanotechnology*, August, 2004.
3. D. B. Newell, J. A. Kramar, J.R. Pratt, D. T. Smith, and E. R. Williams, 2003, "The NIST Microforce Realization and Measurement Project," *IEEE Transactions on Instrumentation and Measurement*, Special issue on CPEM 2002, **52**(2), 2003, pp. 508-511.
4. J. A. Kramar, D. B. Newell, J. R. Pratt, 2002, "NIST Electrostatic Force Balance Experiment," *Proceedings of the joint international conference IMEKO TC3/TC5/TC20*, VDI-Berichte 1685, pp. 71-76.
5. Newell, D.B., Pratt, J.R., Kramar, J.A., Smith, D.T., Feeney, L.A., and Williams, E.R., "SI Traceability of Force at the Nanonewton Level," *Proc. Natl. Conf. of Stds Labs. Intl. 2001 Workshop and Symp.*, Washington, D.C., 2001.
6. Jon R. Pratt, David B. Newell, and John A. Kramar, 2002, "A Flexure Balance with Adjustable Restoring Torque for Nanonewton Force Measurement," *Proceedings of the joint international conference IMEKO TC3/TC5/TC20*, VDI-Berichte 1685, pp. 77-82.
7. Differential Plane Mirror Interferometer, Zygo Model 7015, ZMI Optics guide, p. 2-11, Zygo Corp., Connecticut.
8. J.B. Camp, T.W. Darling, and R. E. Brown, 1991, "Macroscopic variations of surface potentials of conductors," *J. Appl. Phys.*, **69**(10), pp. 7126-7129.
9. J. R. Pratt, D.T. Smith, D.B. Newell, J.A. Kramar, and E. Whinton, 2004, "Progress towards Systeme International d'Unites traceable force metrology for nanomechanics", *Journal of Materials Research*, **19**(1), pp. 366-379.